

## New grids of ATLAS9 atmospheres

### II. Limb-darkening coefficients for the Strömgren photometric system for A-F stars<sup>\*</sup>

C. Barban<sup>1,2</sup>, M. J. Goupil<sup>2</sup>, C. Van't Veer-Menneret<sup>2</sup>, R. Garrido<sup>3</sup>, F. Kupka<sup>4,5</sup>, and U. Heiter<sup>6</sup>

<sup>1</sup> National Solar Observatory, 950 N. Cherry Ave., Tucson, AZ 85719, USA  
e-mail: barban@noao.edu

<sup>2</sup> Observatoire de Paris-Meudon, 5 place Jules Janssen, 92195 Meudon Cedex, France  
e-mail: Caroline.Barban@obspm.fr; MarieJo.Goupil@obspm.fr; Claude.VantVeer@obspm.fr

<sup>3</sup> Instituto de Astrofísica de Andalucía, CSIC, Apdo. 3004, 18080 Granada, Spain  
e-mail: garrido@iaa.es

<sup>4</sup> Astronomy Unit, School of Mathematical Sciences, Queen Mary, University of London Mile End Road, London E1 4NS, UK  
e-mail: f.kupka@qmul.ac.uk

<sup>5</sup> Institut für Astronomie, Universität Wien, Türkenschanzstraße 17, 1180 Vienna, Austria

<sup>6</sup> Department of Astronomy, Case Western Reserve University, 10900 Euclid Ave., Cleveland, OH 44106-7215, USA  
e-mail: ulrike@fafnir.astr.cwru.edu

Received 6 March 2003 / Accepted 16 April 2003

**Abstract.** Using up-to-date model atmospheres (Heiter et al. 2002) with the turbulent convection approach developed by Canuto et al. (1996, CGM), quadratic, cubic and square root limb darkening coefficients (LDC) are calculated with a least square fit method for the Strömgren photometric system. This is done for a sample of solar metallicity models with effective temperatures between 6000 and 8500 K and with  $\log g$  between 2.5 and 4.5. A comparison is made between these LDC and the ones computed from model atmospheres using the classical mixing length prescription with a mixing length parameter  $\alpha = 1.25$  and  $\alpha = 0.5$ . For CGM model atmospheres, the law which reproduces better the model intensity is found to be the square root one for the  $u$  band and the cubic law for the  $v$  band. The results are more complex for the  $b$  and  $y$  bands depending on the temperature and gravity of the model. Similar conclusions are reached for MLT  $\alpha = 0.5$  models. As expected much larger differences are found between CGM and MLT with  $\alpha = 1.25$ . In a second part, the weighted limb-darkening integrals,  $b_\ell$ , and their derivatives with respect to temperature and gravity, are then computed using the best limb-darkening law. These integrals are known to be very important in the context of photometric mode identification of non-radial pulsating stars. The effect of convection treatment on these quantities is discussed and as expected differences in the  $b_\ell$  coefficients and derivatives computed with CGM and MLT  $\alpha = 0.5$  are much smaller than differences obtained between computations with CGM and MLT  $\alpha = 1.25$ .

**Key words.** stars: atmospheres – stars: oscillations – convection

### 1. Introduction

Limb darkening is a well-known effect in stellar atmospheres. It plays an important role in different fields of astrophysics, such as light curve analyses of eclipsing binary systems (e.g. Van Hamme 1993) or, more recently, detections of extra-solar planets by transit (e.g. Mazeh et al. 2000).

Another need for accurate limb darkening coefficients (LDC) is in the field of asteroseismology. LDC are used by methods based on multicolor photometry for oscillation mode identification in variable main sequence stars such as  $\delta$  Scuti and  $\gamma$  Doradus stars (Balona & Evers 1999; Garrido 2000 and references therein; Balona & Dziembowski 1999; Daszynska-Daszkiewicz et al. 2002). These methods involve apparent oscillation amplitudes and phases which need to be precisely calculated. To this end, it is necessary to compute, from model atmospheres, accurate colors and more importantly accurate derivatives of colors, color indices and weighted limb darkening integrals with respect to  $\log T_{\text{eff}}$  and  $\log g$  (Sect. 4, see also Garrido 2000). New grids of stellar

---

Send offprint requests to: C. Barban,  
e-mail: Caroline.Barban@obspm.fr

\* Table 1 is only available in electronic form at the CDS via anonymous ftp to cdsarc.u-strasbg.fr (130.79.128.5) or via <http://cdsweb.u-strasbg.fr/cgi-bin/qcat?J/A+A/405/1095>

atmospheres which fulfill this requirement are now available; they were computed with modified versions of the ATLAS9 code with a higher resolution in optical depth for a more accurate description of the vertical structure of the atmospheres and with a finer grid in the  $(T_{\text{eff}}, \log g)$  plane. Several sets of model atmospheres were computed with different treatments of the convective energy transport (Heiter et al. 2002, hereafter Paper I). LDC computed from these new models with the  $\alpha = 0.5$  MLT (mixing length theory) prescription have already been used for oscillation mode identification purposes (Garrido et al. 2002a,b; Breger et al. 2002) and for the computation of apparent oscillation amplitudes for simulating  $\delta$  Scuti oscillations spectra (Barban et al. 2001).

The purpose of the present paper therefore is twofold: first, we compute LDC for a set of up-dated model atmospheres which have been computed with the turbulent convection approach developed by Canuto et al. (1996, CGM). This approach permits to match a larger amount of observed data, in particular concerning photometry and spectroscopy of A stars (Paper I, for the latter see also Smalley & Kupka 1997 and Smalley et al. 2002). In a second part, we calculate weighted limb darkening integrals as accurate as required for asteroseismic studies. We also compare the results to LDC computed with the MLT convective option with two values of the mixing length parameter  $\alpha = 0.5$  and  $\alpha = 1.25$ . The lower value corresponds to a best representation of at least the first two Balmer Line Profiles in the series using a unique convection model (Van't Veer-Menneret & Mégessier 1996; Fuhrmann et al. 1993; Barklem et al. 2002). The larger value is the Kurucz standard one (Kurucz 1993; Castelli et al. 1997). Balona & Evers (1999) already pointed out the effect of the convective treatment for temperatures below  $\sim 8300$  K on two quantities (the non-adiabatic parameter  $f$  which is the ratio of local luminosity amplitude to displacement amplitude and the phase difference between maximum temperature and maximum radius displacement) which are used to compute the apparent oscillation amplitudes and phases. We will study here this effect on the weighted limb-darkening integrals which are also used to compute the apparent oscillation amplitudes and phases.

For each model atmosphere, the intensity variation over the disk,  $I(\mu)$  (where  $\mu = \cos(\theta)$  and  $\theta$  is the angle between the line of sight and the normal to the local stellar surface) is obtained from solving the transfer equation (hereafter ATLAS9 intensities). In practice, however, it is often more convenient to use intensity variations over the disk which are represented by a  $\mu$ -dependent law, denoted here  $I_{\text{fit}}(\mu)$ . The associated LDC are then obtained by fitting the law  $I_{\text{fit}}(\mu)$  to the model atmosphere intensity variation  $I(\mu)$ . The law to be used is however still debated. The first investigated law was linearly  $\mu$ -dependent (Milne 1921). It was shown that this law is not adequate except for a specific range of effective temperatures around the solar one, i.e. of the order of 5000 K (see Claret 2000 and references therein). Then several other laws were suggested such as laws with a quadratic  $\mu$ -dependence (e.g. Wade & Rucinski 1985; Claret & Giménez 1990), with a square root one (e.g. Díaz-Cordovés & Giménez 1992), with a cubic one (Van't Veer 1960) or with a more sophisticated non-linear  $\mu$ -dependence (Claret 2000).

It is known that the LDC depend on the effective temperature and gravity of the model atmosphere and on the wavelength. In this paper, we focus on stars with convective envelopes with effective temperatures in the range 6000 K–8500 K and surface gravity,  $\log g$ , 2.5–4.5 (the surface gravities are given in CGS units throughout the paper). This range corresponds to stellar parameters of A–F stars of interest here. As mode identification in asteroseismology usually works in Strömgren photometry, we concentrate on these filters. For this range of temperatures and gravities and for the *uvby* bands, Díaz-Cordovés et al. (1995) found that the square root law can be a very good approximation; however, they mentioned that the results may not be conclusive because of the treatment of convection in the model atmospheres. We therefore investigate several laws known to be appropriate for model atmospheres in our range of interest.

The paper is organized as follows: in Sect. 2, we present the model atmospheres we used and their intensity and flux computed in the Strömgren photometric systems. Section 3 is devoted to the computation of the LDC using different limb darkening laws with a discussion of how we select the best law. The resulting LDC are then used to compute the weighted limb-darkening integrals and their derivatives (Sect. 4). The effect of the convection treatment on LDC and on weighted limb-darkening integrals and their derivatives are discussed in Sect. 5. Finally, Sect. 6 is devoted to discussions and conclusions.

## 2. Intensities and fluxes from model atmospheres

A description of the CGM model atmospheres used in this paper is given in Paper I. Our set has a solar chemical composition and covers a range of effective temperatures from 6000 to 8500 K with a step width of 250 K as well as surface gravities,  $\log g$ , from 2.5 to 4.5 with a step width of 0.1 and a microturbulent velocity of  $2 \text{ km s}^{-1}$ .

For studying the effect of convection treatment on limb-darkening, we use also models with the classical MLT convective treatment and for two different values of the mixing length parameter. As in Paper I and for the same reasons, we take the values of the mixing length parameter to be either  $\alpha = 0.5 H_p$  or  $\alpha = 1.25 H_p$  where  $H_p$  is the pressure scale height. All other assumptions in building the model atmospheres are the same for the three different grids.

For each model, monochromatic specific intensities,  $I(\lambda, \mu)$ , are computed for 1221 different values of wavelength at 20 equally spaced values of  $\mu$  from 0.05 to 1 with a step of 0.05. These specific intensities are then integrated over  $\lambda$  for each *u, v, b, y* band:

$$I_x(\mu) = \int_{\lambda_1}^{\lambda_2} I(\lambda, \mu) S_x(\lambda) d\lambda \quad (1)$$

where  $I_x(\mu)$  is the specific intensity in the band *x*;  $I(\lambda, \mu)$  is the monochromatic specific intensity given by the model atmospheres;  $\lambda_1$  and  $\lambda_2$  are the photometric band lower and upper boundaries defining the band *x*.  $S_x(\lambda)$  is the response function for the passband *x* computed in the Kurucz program (Kurucz 1998) of *uvby* colors calculations from ATLAS9 fluxes.

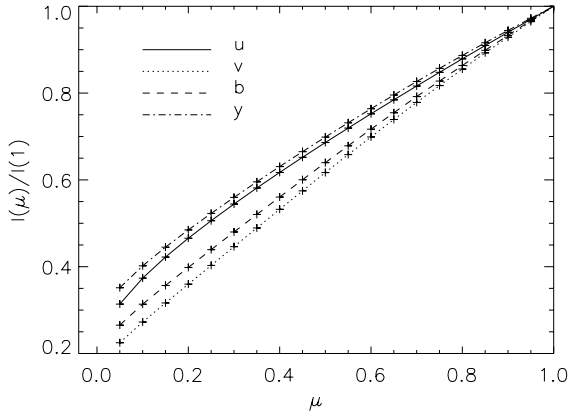


**Fig. 1.**  $I(\mu)/I(1)$  as a function of  $\mu$  for  $\log g = 4.0$ ,  $T_{\text{eff}} = 7250$  K, for  $u, v, b, y$  bands and a CGM model atmosphere.

As explained in Kurucz (1979, references therein), the response function computation includes atmospheric transmissivity, reflection from aluminium mirrors, a standard detector sensitivity, and the filter transmission curves (Matsushima 1969). The response is normalized such that:

$$\int_{\lambda_1}^{\lambda_2} S_x(\lambda) d\lambda = 1.$$

An example of the intensity computed in the Strömgren photometric system is given in Fig. 1. Differences can be seen in the behavior of the intensity with the band because opacities – and consequently optical depth and formation depth – are functions of wavelength. We can then anticipate that the limb-darkening laws which fit best the intensity will differ from one Strömgren band to another.

The flux  $F(\lambda)$  is another output of ATLAS9. It is also integrated over  $\lambda$  for each  $u, v, b, y$  band:

$$F_x = \int_{\lambda_1}^{\lambda_2} F(\lambda) S(\lambda) d\lambda. \quad (2)$$

Figure 2 displays the flux integrated over the Strömgren photometric bands. Díaz-Cordovés et al. (1995) reported a discontinuity in the variation of  $F/I(1)$  with the effective temperature around 7900 K. Claret (2000) and Claret et al. (1995) have shown this discontinuity in the LDC and Claret (2000) attributed this gap to the onset of convection. This discontinuity is due to the use of an overshooting treatment for the top of the hydrogen convection zone in the ATLAS9 code as discussed in Van't Veer & Mégessier (1996) and Castelli et al. (1997) and Castelli (1999). No such discontinuity is visible in our data (see Fig. 2) because in our models, no overshooting is included.

The behavior of the flux in the  $u$  band with the effective temperature differs significantly from that of the other bands. Indeed, the  $u$  band forms much higher in the atmosphere than the other bands.

### 3. Limb-darkening laws and coefficients

#### 3.1. Limb-darkening laws

For our  $T_{\text{eff}}$  and  $\log g$  range of interest, we consider three different laws: quadratic, cubic and square root laws.

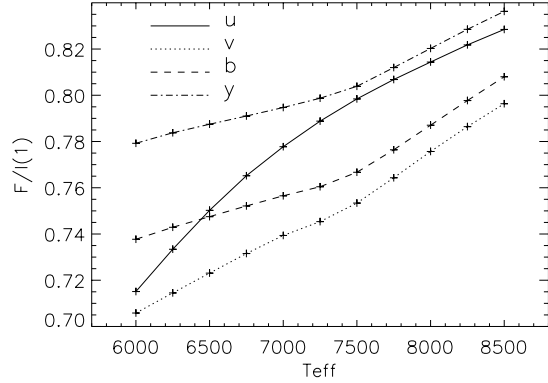


**Fig. 2.**  $F/I(1)$  as a function of  $T_{\text{eff}}$  for  $\log g = 4.0$ , for  $u, v, b, y$  bands and for CGM model atmospheres.

We study these laws for the following forms:

Quadratic law:

$$\left( \frac{I_x(\mu)}{I_x(1)} \right)_{\text{fit}} = 1 - a(1 - \mu) - b(1 - \mu)^2. \quad (3)$$

Cubic law:

$$\left( \frac{I_x(\mu)}{I_x(1)} \right)_{\text{fit}} = 1 - c(1 - \mu) - d(1 - \mu)^2 - e(1 - \mu)^3 \quad (4)$$

which generalizes the cubic law studied by Van't Veer (1960) who considered the case  $d = 0$ .

Square root law:

$$\left( \frac{I_x(\mu)}{I_x(1)} \right)_{\text{fit}} = 1 - f(1 - \mu) - g(1 - \sqrt{\mu}) \quad (5)$$

where  $I_x(1)$  is the specific intensity at the center of the disk for the  $x$  band and  $a, b, c, d, e, f$ , and  $g$  are the corresponding LDC.

#### 3.2. Limb-darkening coefficients

Following e.g. Díaz-Cordovés et al. (1995), we choose a least-square method (LSM) as the numerical method to compute the LDC. We therefore obtain the LDC for the three different limb-darkening laws (Eqs. (3)–(5)) by determining the best fit between the considered law and the ATLAS9 intensities with an LSM. Several works (e.g. Díaz-Cordovés et al. 1995; Claret 2000) have shown that this method reproduces better the variation of intensity over the stellar disk than the method which is based on the flux conservation as used, e.g., by Wade & Ruciński (1985).

Limb-darkening coefficients for the three laws and for the  $u$  band are given in Table 1 for our temperature and gravity ranges; the corresponding standard deviation  $\sigma$  for each law is also given as an indication of the quality of the fit.  $\sigma$  is defined as:

$$\sigma^2 = \frac{1}{N} \sum_{i=1}^N \left[ \frac{I(\mu_i)}{I(1)} - \left( \frac{I(\mu_i)}{I(1)} \right)_{\text{fit}} \right]^2 \quad (6)$$

where  $N$  is the number of  $\mu$  values, here  $N = 20$ . The data for the other bands are available on [http://dasgal.obspm.fr/~barban/Limb\\_AF/](http://dasgal.obspm.fr/~barban/Limb_AF/). With the adopted numerical scheme, accuracy of the calculation is  $\sim 2\%$ – $10\%$  depending on the band,

or equivalently two digits in the numerical values of the coefficients are significant; Table 1 nevertheless lists them with 3 digits for comparison with results of previous authors.

Figure 3 represents the LDC for each law at a given gravity as a function of temperature and for the Strömgren photometric bands. The coefficients  $a$  to  $g$  behave smoothly with effective temperature. Gaps or discontinuities are not seen, for the same reason as discussed in Sect. 2. Whatever the band, the linear coefficient is dominant for the 3 laws (except for the square root law at high temperatures). This explains why the linear coefficients  $a$ ,  $c$ ,  $f$  behave the same way i.e. decrease with the effective temperature as expected (see Díaz-Cordovés et al. 1995 and references therein). The corrective term coefficients (quadratic and square root)  $b$  and  $g$  vary in a similar way with the effective temperature. Coefficients  $d$  and  $e$  behave differently than the  $b$  and  $g$  coefficients as compensating effects can exist when two corrective terms are used (in the cubic law) instead of one (quadratic and square root laws).

Like for the flux (Fig. 2), the effective temperature dependence of coefficients in the  $u$  band is quite different from the other bands. The three other bands on the other hand show a similar effective temperature dependence.

### 3.3. Selecting the best limb-darkening laws

The limb-darkening law must represent well enough the model atmosphere intensity variation over the disk. To quantify the quality of the fit between the model atmosphere intensity and the given law, we followed Díaz-Cordovés & Giménez (1992) and used the standard deviation,  $\sigma$  (see Eq. (6)). For the 4 photometric bands and the considered range of temperature and gravity,  $\sigma$  remains smaller than  $\sim 1.3 \times 10^{-2}$ . Figure 4 is a typical example of  $\sigma$  values found for our temperature range, for  $\log g = 4.0$ , and the Strömgren photometric bands. Figure 4 confirms that the law which best reproduces the model atmosphere intensity depends on the photometric band and on the effective temperature. For this particular example, the square root law clearly gives the best result for the  $u$  band, the cubic law for the  $v$  band. For the other bands,  $b$  and  $y$ , no general rule can be drawn; any of the three laws can give the smaller  $\sigma$  depending on the effective temperature and gravity.

Another indication of the goodness of the fit is the comparison between the variation with  $\mu$  of the ATLAS9 intensity and that of the intensity derived from the limb-darkening law. Figure 5 displays such a comparison for a given temperature and gravity. This figure shows that, for a given temperature and gravity, the square root law gives the best result for the  $u$  band while it is the cubic law which gives the best result for the other 3 bands. It must be noted that for the  $b$  band, the cubic and quadratic law give the same result (cf. also Fig. 4).

In practice, we use the  $\sigma$  criterion for selecting the best law but check also that the variation of the intensities with  $\mu$  is correctly reproduced. With a tolerance of  $\delta\sigma = 0.001$  in the  $\sigma$ 's that are given in Table 1 (i.e. two laws are considered of similar quality whenever their  $\sigma$ 's differ by less than 0.001), we find a unique best law for each band,  $u$  and  $v$ , for our temperature and gravity ranges. Hence in the remainder of the paper, the

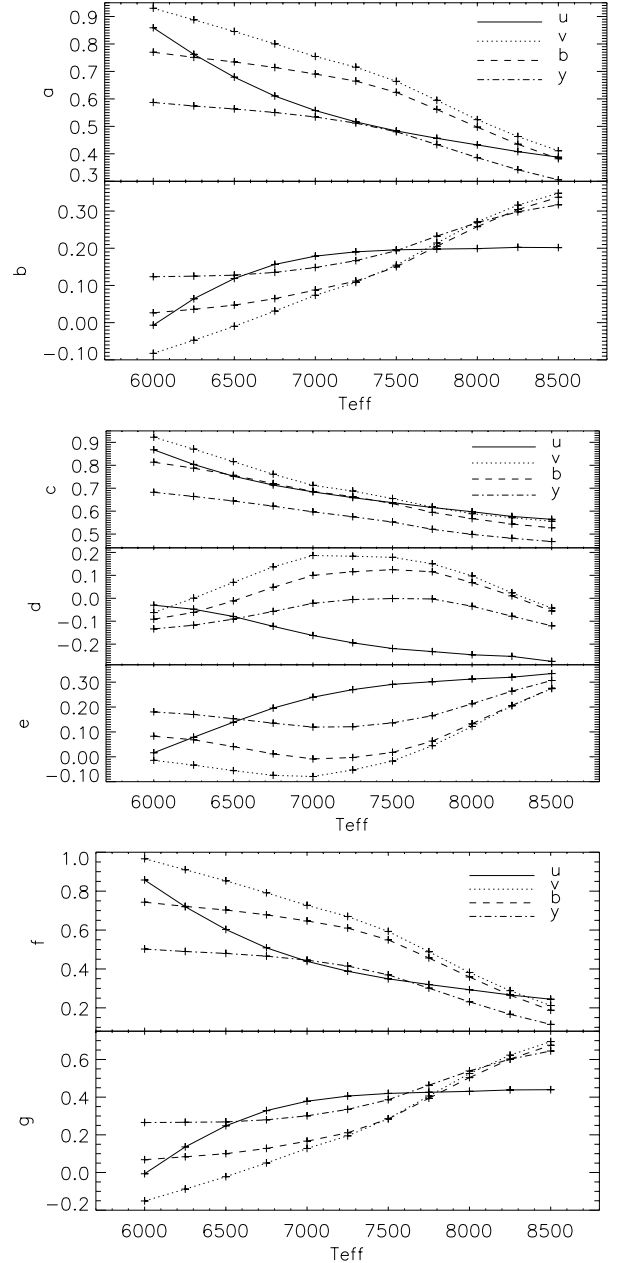


**Fig. 3.** The quadratic coefficients,  $a$  and  $b$ , the cubic coefficients,  $c$ ,  $d$  and  $e$ , and the square root coefficients,  $f$  and  $g$ , as a function of temperature, for  $\log g = 4.0$ , for  $uvby$  bands and for CGM models.

square root law is chosen as the best law for the  $u$  band and the cubic law for the  $v$  band. For the  $b$  band, the best law can be taken as the cubic one for all temperatures and gravities except for some high gravities at low temperatures (at 6000 K with  $\log g = 4.3$  and 4.5 and at 6250 K with  $\log g = 3.8$ –4.5) for which we must take the square root law. For the  $y$  band, the cubic law is selected except for some gravities and effective temperatures for which we must choose the square root law (at 6000 K and 6250 K with all  $\log g$ , at 6500 K with  $\log g = 3$ –4.5 and at 6750 K with  $\log g = 4.3$ –4.5). For any band, the best law yields a  $\sigma$  smaller than 0.003–0.004. As a consequence, it turns out that the quadratic law is not selected in the effective temperature and gravity range of interest here.

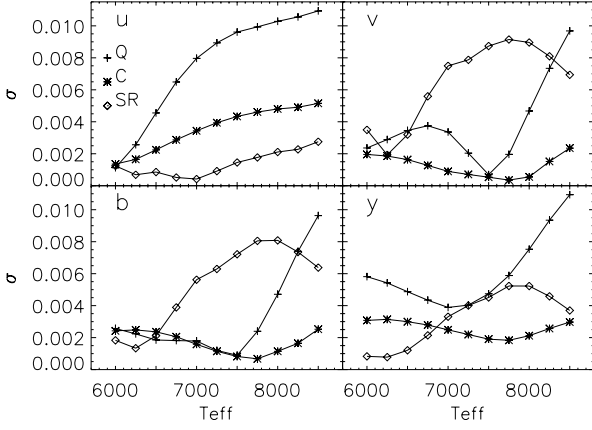


**Fig. 4.**  $\sigma$  as a function of temperature for  $\log g = 4.0$ , for the *uvby* bands and for CGM models. + correspond to the quadratic law (Q), \* to the cubic law (C), and  $\diamond$  to the square root law (SR).

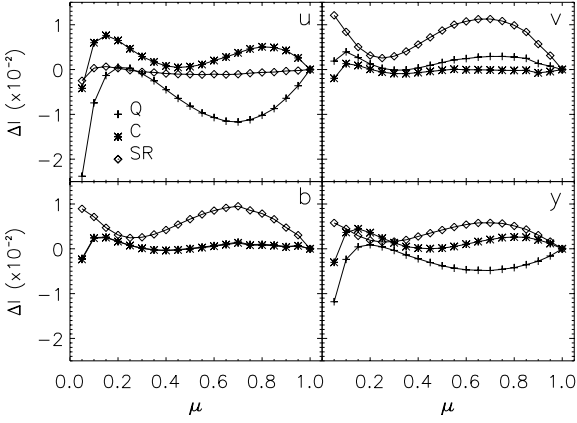


**Fig. 5.**  $\Delta I \equiv I(\mu)/I(1) - I(\mu)/I(1)_{\text{law}}$  as a function of  $\mu$  for  $T_{\text{eff}} = 7250$  K and  $\log g = 4.0$ , for the *uvby* bands and for CGM models. + corresponds to the quadratic law, \* to the cubic law, and  $\diamond$  to the square root law.

Once the best law is selected and for the four bands, the flux computed with the limb-darkening laws fits the ATLAS9 flux to better than 0.45% and the intensity variation over the disk computed with limb-darkening laws to better than 3.5% at low  $\mu$  and than 0.5% for  $\mu$  greater than 0.2.

#### 4. Weighted limb-darkening integrals

Photometric methods for oscillation mode identification which are currently used for  $\delta$  Scuti and  $\gamma$  Doradus stars are based on an analytic expression for the flux variation due to non radial pulsation (Watson 1988 and for instance Balona & Dziembowski 1999). This expression uses weighted limb darkening integrals and their derivatives with respect to  $\log T_{\text{eff}}$  and  $\log g$ . The weighted limb darkening integrals are defined as:

$$b_{\ell x} = \int_0^1 h_x(\mu) \mu P_\ell(\mu) d\mu \quad (7)$$

where:

-  $P_\ell$  are the Legendre polynomials of order  $\ell$ ;

-  $h_x(\mu)$  is the limb-darkening function, defined as:

$$h_x(\mu) = h_x(1) \left( \frac{I_x(\mu)}{I_x(1)} \right)_{\text{fit}} \quad \text{with} \quad h_x(1) = 2 \frac{I_x(1)}{F_x} \quad (8)$$

where  $F_x$  is the model atmosphere flux in the  $x$  band.  $h_x(\mu)$  is normalized as (Watson 1988):

$$\int_0^1 \mu h_x(\mu) d\mu = 1. \quad (9)$$

We find it convenient to rewrite the limb darkening laws (Eq. (3)–(5)) under the forms:

- for the quadratic law:

$$h_x(\mu) = X_{0,x} + X_{1,x}\mu + X_{2,x}\mu^2 \quad (10)$$

- for the cubic law:

$$h_x(\mu) = Y_{0,x} + Y_{1,x}\mu + Y_{2,x}\mu^2 + Y_{3,x}\mu^3 \quad (11)$$

- for the square root law:

$$h_x(\mu) = Z_{0,x} + Z_{1,x}\mu + Z_{2,x}\sqrt{\mu} \quad (12)$$

where  $X_{i,x}$ ,  $Y_{i,x}$ ,  $Z_{i,x}$  are constants and depend on the physics of the model atmosphere and on the  $x$  band. The normalization condition (Eq. (9)) imposes the following relations:

- for the quadratic law:

$$X_{0,x} = 2 - \frac{2}{3} X_{1,x} - \frac{1}{2} X_{2,x} \quad (13)$$

- for the cubic law:

$$Y_{0,x} = 2 - \frac{2}{3} Y_{1,x} - \frac{1}{2} Y_{2,x} - \frac{2}{5} Y_{3,x} \quad (14)$$

- for the square root law:

$$Z_{0,x} = 2 - \frac{2}{3} Z_{1,x} - \frac{4}{5} Z_{2,x}. \quad (15)$$

Substituting Eqs. (10)–(12) into Eq. (7) and using Eqs. (13)–(15) gives:

- for the quadratic law:

$$b_{\ell x} = C_{0,\ell} + C_{1,\ell} X_{1,x} + C_{2,\ell} X_{2,x} \quad (16)$$

- for the cubic law:

$$b_{\ell x} = C_{0,\ell} + C_{1,\ell} Y_{1,x} + C_{2,\ell} Y_{2,x} + C_{3,\ell} Y_{3,x} \quad (17)$$

- for the square root law:

$$b_{\ell x} = C_{0,\ell} + C_{1,\ell} Z_{1,x} + C'_{2,\ell} Z_{2,x}. \quad (18)$$

The coefficients  $C_{i,\ell}$  are then given by

$$\begin{aligned} C_{0,\ell} &= 2 I_{\ell,1} \\ C_{1,\ell} &= I_{\ell,2} - (2/3) I_{\ell,1} \\ C_{2,\ell} &= I_{\ell,3} - (1/2) I_{\ell,1} \\ C_{3,\ell} &= I_{\ell,4} - (2/5) I_{\ell,1} \\ C'_{2,\ell} &= I_{\ell,3/2} - (4/5) I_{\ell,1} \end{aligned} \quad (19)$$

where following Dziembowski (1977), we define:

$$I_{\ell,q} = \int_0^1 \mu^q P_\ell(\mu) d\mu. \quad (20)$$

Table 2 lists the  $C_{i,\ell}$  coefficients for  $\ell = 0-10$ . The  $X_i, Y_i, Z_i$  quantities are related to the LDC  $a$  to  $g$  (Eqs. (3)–(5) and (8)) by:

$$\begin{aligned} X_{1,x} &= h_x(1) (a + 2b), & X_{2,x} &= -h_x(1) b \\ Y_{1,x} &= h_x(1) (c + 2d + 3e), & Y_{2,x} &= -h_x(1) (d + 3e) \\ Y_{3,x} &= h_x(1) e \\ Z_{1,x} &= h_x(1) f, & Z_{2,x} &= h_x(1) g. \end{aligned}$$

An example of variation of  $h_x(1)$  with effective temperature for a given gravity can be seen from Fig. 2.

The derivatives of  $b_{\ell,x}$  with respect to  $\log T_{\text{eff}}$  and  $\log g$  are numerically computed by means of a cubic spline decomposition and care has been taken to avoid grid boundary effects.

For later discussion, we note that a general variation of  $b_{\ell,x}$  can be written for the square root law (Eq. (18)), for instance, as:

$$\Delta b_{\ell,x} = C_{1,\ell} \Delta Z_{1,x} + C'_{2,\ell} \Delta Z_{2,x} \quad (21)$$

where  $\Delta$  represents either a derivative with respect to  $\log T_{\text{eff}}$  or to  $\log g$  or represents the difference between  $b_{\ell,x}$  computed with two different assumptions for the convective treatment of the model atmosphere.

Hence, dependences of the  $b_{\ell,x}$  in Eq. (16)–(18) of their derivatives or variations in Eq. (21) with convection depend on one hand on  $\ell$  through the  $I_{\ell,q}$  ( $C_{i,\ell}$ ) and on the other hand on  $\log T_{\text{eff}}$ ,  $\log g$ , and on the convection model (through the structure of the atmosphere) through the coefficients  $X, Y$ , and  $Z$ .

#### 4.1. Dependence of $b_\ell$ and derivatives on the limb darkening law

Here, we compare the  $b_\ell$  coefficients computed with the cubic and square root laws. Differences in the  $b_\ell$  between these two laws are negligible at low  $\ell$  (smaller than 0.1% for  $\ell < 3$ ) and tend to increase with the degree  $\ell$  and, for instance, reach up to 15% for  $\ell = 5, 6$  in the  $u$  band and 50% in the  $v$  band. The differences significantly depend on  $T_{\text{eff}}$  but show a similar behavior with gravity changes. This remains true for any  $\ell$ .

The  $b_\ell$  derivatives are also sensitive to the choice of the limb darkening law. Differences in the derivatives with respect to  $\log T_{\text{eff}}$  are significant for  $\ell > 4$  and are present mainly at low temperatures ( $T_{\text{eff}} < 7500$  K). Differences in the derivatives with respect to  $\log g$  can differ by a factor 4–5 for  $\ell > 4$ , but nevertheless remain small as the derivatives themselves are small.

We have shown here that except for low  $\ell$  values, the effect of the limb darkening law on  $b_\ell$  and their derivatives is not negligible.

#### 4.2. Dependence of $b_\ell$ and derivatives on temperature and gravity

The weighted limb-darkening integrals are computed with a limb darkening law which is selected as the best one

**Table 2.**  $C_{i,\ell}$  coefficients for  $\ell = 0$  to 10 for quadratic, cubic, and square root laws.

$\ell$	$C_0$	$C_1$	$C_2$	$C'_2$	$C_3$
0	+1	0	0	0	0
1	2/3	1/36	1/30	2/105	1/30
2	1/4	1/20	1/16	1/30	9/140
3	0	1/24	2/35	2/77	1/16
4	-1/24	1/72	5/192	1/156	17/504
5	0	-1/192	0	-2/385	1/160
6	1/64	-1/192	-7/1280	-343/106080	-1/320
7	0	1/640	0	2/1045	-1/1920
8	-1/128	1/384	3/1280	907/495040	1/640
9	0	-1/1536	0	-2/2185	1/8960
10	7/1536	-7/4608	-55/43008	-2629/2284800	-7/7680

according to the Sect. 3.3, that-is, for instance, the square root law for the  $u$  band and the cubic law for the  $v$  band.

The  $b_\ell$  are only weakly dependent on  $T_{\text{eff}}$  and  $\log g$ . On the other hand, their derivatives significantly depend on  $\log g$  and on  $T_{\text{eff}}$ . These dependencies are  $\ell$ -dependent and differ in each  $u, v, b, y$  band (see Figs. 6 and 7).

##### 4.2.1. A typical low $\ell$ case

Figure 6 illustrates a typical low  $\ell$  case, i.e.  $\ell = 3$ . The  $b_{\ell=3,x}$  coefficients and their derivatives with respect to  $\log g$  and  $\log T_{\text{eff}}$  are plotted versus  $T_{\text{eff}}$  and for different values of  $\log g$ . Only the coefficients for  $u$  and  $v$  bands are shown as those for the  $b$  and  $y$  bands behave quite similarly to the  $v$  coefficients.

For the  $u$  band (and the square root law),  $b_{\ell=3,x}$  decreases with  $T_{\text{eff}}$  and increases with  $\log g$ . Its derivatives with respect to  $\log T_{\text{eff}}$  monotonously increase with  $T_{\text{eff}}$  and decrease with  $\log g$ . Derivatives of  $b_\ell$  with respect to the gravity are about 2 orders of magnitude smaller than the derivatives of  $b_\ell$  with  $T_{\text{eff}}$  and are more sensitive to numerical accuracy limitations.

The  $b_{\ell=3,x}$  for the other bands decrease monotonously and smoothly with  $T_{\text{eff}}$ . On the other hand, the  $b_{\ell=3,x}$  in  $v, b$ , and  $y$  bands decrease with  $\log g$  in contrast with the  $b_{\ell=3,x}$  behavior in the  $u$  band. This is directly related to the different behavior of the intensities in the band  $u$  compared to the other bands with  $T_{\text{eff}}$  (see Fig. 1). Derivatives of  $b_{\ell=3,x}$  in the other bands are non-monotonously varying with  $T_{\text{eff}}$  and  $\log g$  and are of the same order of magnitude as for the  $u$  band.

##### 4.2.2. Dependence of $b_\ell$ and derivatives on $\ell$

It is well known that for a given model atmosphere,  $b_\ell$  decreases with  $\ell$  (Dziembowski 1977). Figure 7 shows the  $b_\ell$ 's and their derivatives as a function of  $T_{\text{eff}}$  and  $\log g$  for various  $\ell$  values for the  $u$  band (and the square root law). The  $T_{\text{eff}}$  and  $\log g$  behavior of the  $b_\ell$ 's is similar, i.e. a decrease with  $T_{\text{eff}}$  and an increase with  $\log g$ , for  $\ell = 1$  to 4 and for  $\ell = 7, 8$ . The  $\ell = 5, 6, 10$  both increase with  $T_{\text{eff}}$  and decrease with  $\log g$  while  $\ell = 9$  shows a minimum around 6500 K and decreases with  $\log g$ . The absolute values of the derivatives of  $b_{\ell,x}$  with respect to  $\log g$  and  $\log T_{\text{eff}}$  also decrease rapidly towards small values with increasing degrees (Fig. 7). Derivatives of  $b_\ell$  with

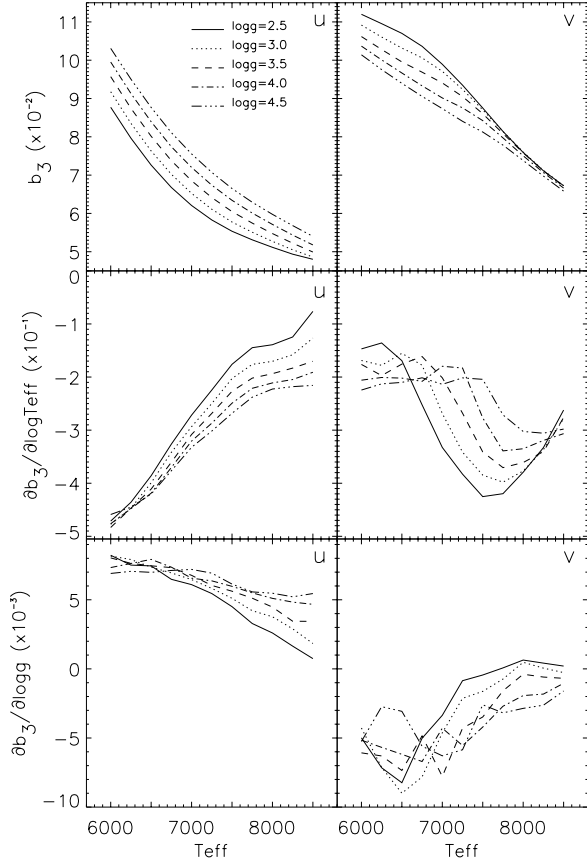


**Fig. 6.** For  $u$  and  $v$  bands and for CGM models; top: weighted limb darkening integrals  $b_{\ell=3}$  (the square root law was used for  $u$ , and the cubic law for  $v$ ); middle: partial derivatives of  $b_{\ell=3}$  with respect to  $\log T_{\text{eff}}$ ; bottom: partial derivatives of  $b_{\ell=3}$  with respect to  $\log g$ .

$\log T_{\text{eff}}$  vary in a similar way with  $T_{\text{eff}}$  for  $\ell = 1$  to 4 and  $\ell = 8$ , decrease for  $\ell = 6, 7$  and show a maximum for  $\ell = 5, 9, 10$  around 7000 K. Derivatives of  $b_{\ell}$  with the gravity remain small: roughly these derivatives amount to  $10^{-3}$  at low  $\ell$  and decrease down to  $10^{-6}$ – $10^{-5}$  at high  $\ell$ . Figure 8 shows  $b_{\ell}$  derivatives for the  $v$  band for several  $\ell$ . This can be explained by the  $\ell$  dependence of the  $b_{\ell}$  derivatives at low  $\ell$  which follows the  $\ell$  behavior of the  $C_{i,\ell}$  coefficients (i.e. the  $I_{\ell,q}$  in Eq. (19)) and differs depending on whether  $\ell - q$  is positive or negative, even or odd (Dziembowski 1977). For instance, for the  $u$  band in Fig. 7 and the  $v$  band in Fig. 8, a qualitative change of behavior in the  $b_{\ell}$  derivatives is seen to occur between  $\ell \leq 2$  and  $\ell > 2$  which arises because  $C_{1,\ell}$  in Eq. (19) involves  $I_{\ell,2}$ . Indeed, from the definition, the expression for  $I_{\ell,q}$  differs for  $\ell > q$  and  $\ell < q$ . Here  $q = 2$  and the behavior of  $I_{\ell,2}$  differs for  $\ell > 2$  and  $\ell < 2$ .

For high  $\ell$ , the integrals  $I_{\ell,q}$  behave as  $\ell^{-(q+3/2)}$  for an integer  $q$  (Dziembowski 1977). For  $q = 3/2$ , we find that

$$I_{\ell,3/2} = (-)^{(\ell-3)/2} \frac{6}{(5+2\ell)(1+2\ell)(2\ell-3)} \quad \text{for odd } \ell$$

$$I_{\ell,3/2} = (-)^{(\ell-2)/2} \frac{6}{(5+2\ell)(1+2\ell)(2\ell-3)} \quad \text{for even } \ell$$

and asymptotically for high  $\ell$ , we therefore also have  $I_{\ell,3/2} \sim \ell^{-3}$ .

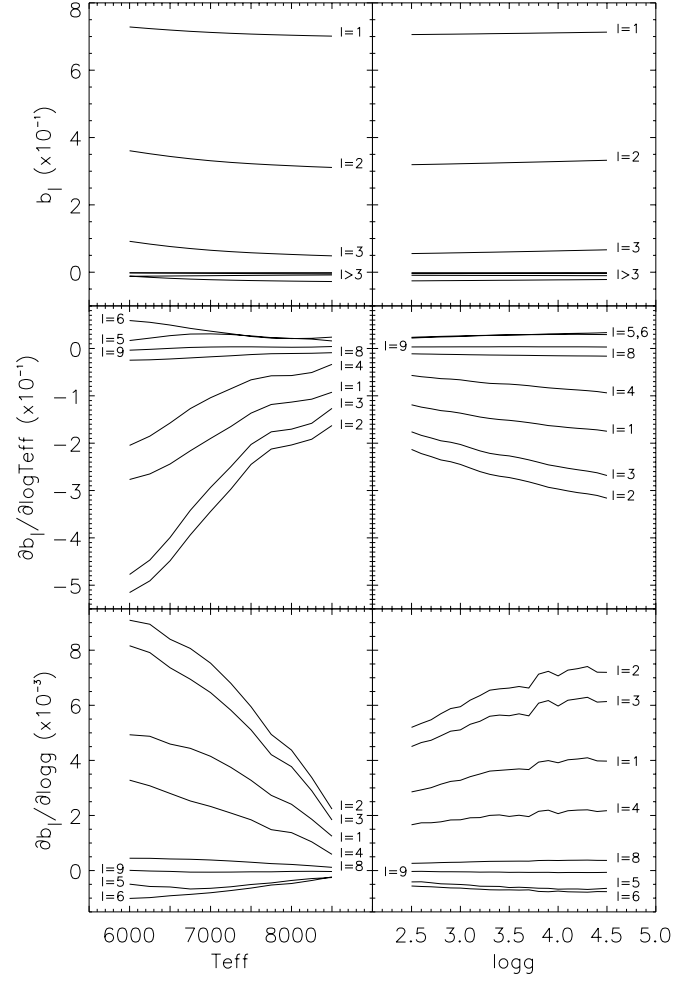


**Fig. 7.** For  $u$  band and for CGM models:  $b_{\ell}$  (top panel) and its derivatives with respect to  $\log T_{\text{eff}}$  (middle) and  $\log g$  (bottom) as a function of  $T_{\text{eff}}$  (left side) for  $\log g = 3.0$  and as a function of  $\log g$  for  $T_{\text{eff}} = 7500$  K (right side), for several  $\ell$  values ( $\ell = 7$  and  $\ell = 10$  would be close to  $\ell = 9$ ).

The high  $\ell$  behavior of the dominant  $C$ 's coefficients (Eqs. (19)–(20)) then is:

for odd  $\ell$ :

$$C_{0,\ell} = 0 = C_{2,\ell} \quad (22)$$

$$C_{1,\ell} \sim 2\sqrt{2/\pi} (-)^{(\ell-3)/2} \ell^{-7/2} \quad (23)$$

$$C'_{2,\ell} \sim \frac{3}{4} (-)^{(\ell-3)/2} \ell^{-3} \quad (24)$$

for even  $\ell$ , one has:

$$C_{1,\ell} = -C_{0,\ell}/3; \quad C_{2,\ell} \sim -C_{0,\ell}/4 \quad (25)$$

$$C_{3,\ell} = -C_{0,\ell}/5; \quad C'_{2,\ell} \sim -2C_{0,\ell}/5 \quad (26)$$

and

$$C_{0,\ell} \sim 2\sqrt{2/\pi} (-)^{(\ell-2)/2} \ell^{-5/2}. \quad (27)$$

Accordingly, for high  $\ell$ , the  $b_{\ell}$  behavior and its derivatives or variations with the physics of the model obeys:

for the cubic law:

- for odd  $\ell$ :

$$b_{\ell} \sim 2\sqrt{2/\pi} (-)^{(\ell-3)/2} \ell^{-7/2} Y_1 \quad (28)$$

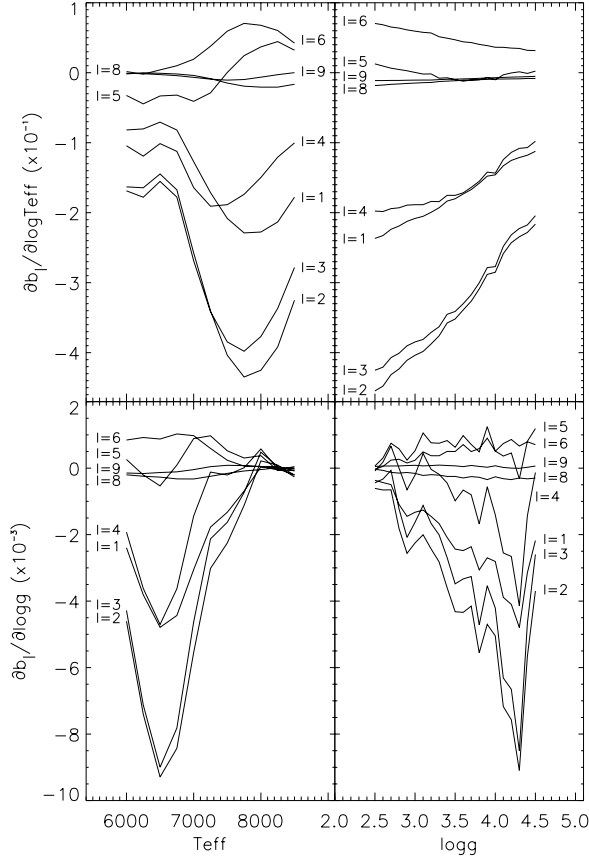


**Fig. 8.** For the  $v$  band and for CGM models: derivatives of  $b_\ell$  with respect to  $\log T_{\text{eff}}$  (top) and  $\log g$  (bottom) as a function of  $T_{\text{eff}}$  (left side) for  $\log g = 3.0$  and as a function of  $\log g$  for  $T_{\text{eff}} = 7500$  K (right side) for several  $\ell$  values ( $\ell = 7$  and  $\ell = 10$  would be close to  $\ell = 9$ ).

$$\Delta b_\ell \sim 2\sqrt{2/\pi} (-)^{(\ell-3)/2} \ell^{-7/2} \Delta Y_1 \quad (29)$$

- for even  $\ell$ :

$$b_\ell \sim C_{0,\ell} \left(1 - \frac{1}{3}Y_1 - \frac{1}{4}Y_2 - \frac{1}{5}Y_3\right) \quad (30)$$

$$\Delta b_\ell \sim -\frac{1}{3}C_{0,\ell} (\Delta Y_1 + \frac{3}{4}\Delta Y_2 + \frac{3}{5}\Delta Y_3) \quad (31)$$

with  $C_{0,\ell}$  given by Eq. (27).

for the square root law:

- for odd  $\ell$ :

$$b_\ell \sim \frac{3}{4} (-)^{(\ell-3)/2} \ell^{-3} Z_2 \quad (32)$$

$$\Delta b_\ell \sim \frac{3}{4} (-)^{(\ell-3)/2} \ell^{-3} \Delta Z_2 \quad (33)$$

- for even  $\ell$ :

$$b_\ell \sim 2\sqrt{2/\pi} (-)^{(\ell-2)/2} \ell^{-5/2} \left(1 - \frac{1}{3}Z_1 - \frac{2}{5}Z_2\right) \quad (34)$$

$$\Delta b_\ell \sim -2\sqrt{2/\pi} (-)^{(\ell-2)/2} \ell^{-5/2} \left(\frac{1}{3}\Delta Z_1 + \frac{2}{5}\Delta Z_2\right) \quad (35)$$

where we have dropped the band subscript  $x$  for clarity.

It must be noted that the  $b_\ell$  behavior at high  $\ell$  is very different depending on whether the degree is even or odd: it decreases more rapidly for odd  $\ell$  than for even  $\ell$  (as already noticed by Dziembowski et al. 1998) for a given law. In addition, for the cubic law, the linear term remains dominant for odd  $\ell$  whereas the corrective terms (higher  $\mu$  dependence of the law) do also contribute for even  $\ell$ . For the square root law, the corrective term (square root  $\mu$  dependence) is dominant for odd  $\ell$  whereas it contributes roughly equally with the other terms for even  $\ell$ .

## 5. Effect of the convective treatment

### 5.1. Limb-darkening coefficients

We now compare the LDC for our CGM models with the LDC which have been computed assuming a classical MLT convective treatment and for two values of the mixing length parameter ( $\alpha = 0.5$  and  $\alpha = 1.25$ ).

As expected largest differences occur between CGM and MLT  $\alpha = 1.25$  whereas differences between CGM and MLT  $\alpha = 0.5$  remain much smaller (see Fig. 9).

For the coefficients  $a$ ,  $c$ , and  $f$  in the  $u$  band, the differences between CGM and MLT  $\alpha = 1.25$  models extend toward higher temperatures for model atmospheres with higher gravities where they reach their maximum value of 10%, i.e. more than the numerical precision of the calculation of the coefficients themselves ( $\sim 2\%$ ). For  $b$ ,  $e$ , and  $g$  in the  $u$  band also, the differences are smaller than 25% except for few points with much higher differences (up to a factor 10); these differences reach their maximum at low temperature. And finally, for the coefficient  $d$  in the  $u$  band, differences are as high as a factor 4 which is reached at low temperature. For the bands  $v$  and  $b$ , the differences for  $a$  and  $c$  are less than 30% and less than 60% for  $f$ . For these three coefficients, the differences extend toward the highest temperatures for model atmospheres with higher gravities. The other coefficients,  $b$ ,  $d$ ,  $e$ , and  $g$ , differ in maximum by a factor  $\sim 20$ – $30$  at low temperature. For the band  $y$ , the values are intermediate between the band  $u$  ones and the  $v$  and  $b$  ones except for the coefficient  $d$  which has the same differences as in the  $v$  and  $b$  bands. For this band, the differences propagate toward higher temperatures for model atmospheres with higher gravities. The band  $u$  is less affected by the treatment of convection than the other bands because it is formed higher in the atmosphere, above the convection zone.

A comparison between LCD computed with MLT  $\alpha = 0.5$  and CGM model atmospheres shows differences which are smaller than the ones mentioned above. They behave as above with largest differences in the bands  $b$ ,  $v$  reaching 10% for  $a$ ,  $c$ , and  $f$  and a factor 8 for the other coefficients. We note however that the coefficient  $d$  stands out, because differences between CGM and MLT  $\alpha = 0.5$  reach the same order of magnitude as the differences between CGM and MLT  $\alpha = 1.25$ ; this happens for models with intermediate gravity and below  $\sim 7600$  K. This can be explained by the fact that the maximum flux for each band happens to be in a region which, when it is convective, is more or less efficient in transporting heat

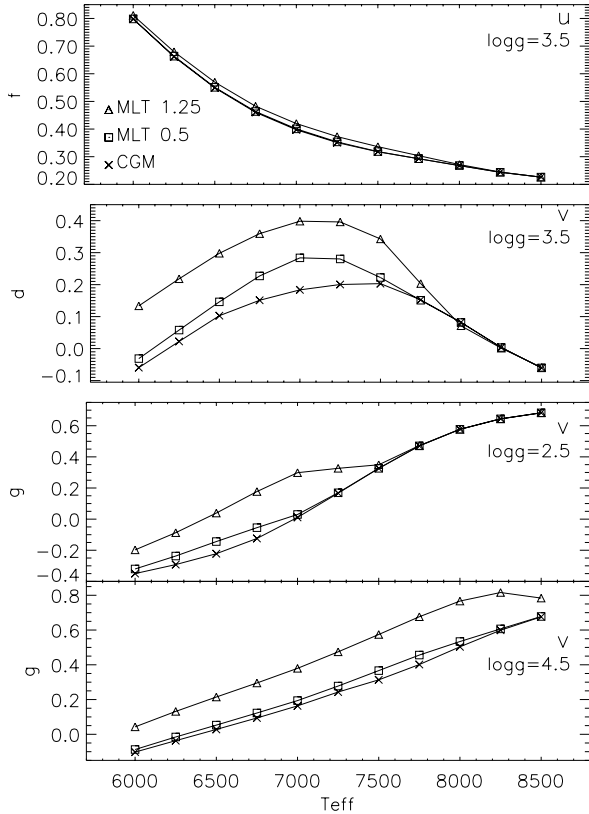


**Fig. 9.** Typical examples of  $f$ ,  $d$ , and  $g$  as a function of  $T_{\text{eff}}$  for a given photometric band for a given value of  $\log g$  and for three different convection options (MLT  $\alpha = 0.5$ , MLT  $\alpha = 1.25$  and CGM).

depending on the adopted convection model and adopted values of the convection parameters.

The above differences in LDC closely follow the differences in the temperature vertical structure of the model atmosphere due to different treatments of the convective energy transport as discussed in Paper I.

### 5.2. Best law for a given band

We now consider the effect of convection treatment in the model atmosphere on the selection of the best law for a given band. Again, there are more differences with CGM models compared with MLT  $\alpha = 1.25$  model atmospheres than with CGM model atmospheres compared with MLT  $\alpha = 0.5$  model atmospheres. With a tolerance  $\delta\sigma = 0.001$  as used above, the law considered as the best is the same with CGM model atmospheres and MLT  $\alpha = 0.5$  model atmospheres except for a couple of models in the  $b$  band (at 6000 K and for  $\log g = 3.8, 4.0\text{--}4.2, 4.4$ ).

The “best” law is the same in the  $v$  band for CGM and MLT  $\alpha = 1.25$  models. For the other bands, many differences exist and no general trend can be established.

### 5.3. Weighted limb-darkening integrals $b_\ell$ and their derivatives

As a general statement, differences in the  $b_\ell$  coefficients and derivatives computed with CGM and MLT  $\alpha = 0.5$  are much smaller than differences obtained between computations with CGM and MLT  $\alpha = 1.25$ , as expected from the above remarks.

Comparisons for some typical cases are shown in Fig. 10. As found earlier (Balona & Evers 1999), differences in the convective treatment disappear at  $\sim 8300$  K above which the temperature gradient is radiative.

The variations (increase or decrease) of the  $b_\ell$  coefficients with  $T_{\text{eff}}$  and  $\log g$  show similar trends for the three convection options. Like for the LDC, the effect is maximal on  $b_\ell$  for low effective temperatures, low gravity model atmospheres, but these large differences extend towards higher temperatures for models with higher gravity. However, the magnitude of the differences is not the same. As can be seen in Fig. 10, the magnitude of the differences in the  $b_\ell$ 's due to the convection treatment is  $\ell$  dependent. It is large for small  $\ell$  and decreases with increasing  $\ell$  due to the  $C_{i,\ell}$  dependence of the  $b_\ell$ . For instance for the  $u$  band, the square root law has been chosen and one has  $\Delta b_{\ell,u} \sim C_{1,\ell} \Delta Z_{1,u} = C_{1,\ell} \Delta(h_u(1) f)$  as  $f$  is dominant over  $g$ .  $\Delta$  here represents the change due to different treatments for the convective flux. Hence  $\Delta b_{\ell,u}$  decreases with  $\ell$  like  $C_{1,\ell}$  for a given change in the  $\Delta Z_{1,u}$ .

The effect, on  $b_\ell$  and derivatives, of changing the convective option in the model atmospheres is dominant in the  $v$  band.

For the effect of convection on the derivatives, we can consider the  $u$  band (and the square root law) as a representative band. Differences between  $\partial b_\ell / \partial \log T_{\text{eff}}$  computed with CGM and MLT  $\alpha = 1.25$  can reach up to 20% whereas differences between  $\partial b_\ell / \partial \log T_{\text{eff}}$  computed with CGM and MLT  $\alpha = 0.5$  reach at maximum 5%.

Derivatives of  $b_\ell$  with the gravity show a similar behavior when computed with CGM and MLT  $\alpha = 0.5$  while computations with MLT  $\alpha = 1.25$  result in values which differ to an extent which depends on  $T_{\text{eff}}$  and gravity. The difference between computations with CGM and MLT  $\alpha = 1.25$  is about  $< 10^{-4}$  for low  $\ell$  and decreases for high  $\ell$ . Differences are much smaller between derivatives computed with CGM and MLT  $\alpha = 0.5$  with a maximum of  $5 \times 10^{-4}$  for low  $\ell$  and  $5 \times 10^{-5}$  for  $\ell = 10$  for instance.

## 6. Discussion and conclusions

LDC have been computed for model atmospheres with a solar metallicity, an effective temperature in the range 6000–8500 K and  $\log g$  in the range 2.5–4.5 with 3 different laws: quadratic, cubic, and square root. Our model atmospheres are built with a turbulent convection approach developed by Canuto et al. (1996, CGM), which is considered as an improvement over the MLT prescription and is implemented today for non-grey, line blanketed, horizontally averaged models.

In order to study the effect on LDC of the treatment of convection, we used also model atmospheres built with the MLT prescription for two different values of  $\alpha$ : 0.5 and 1.25.

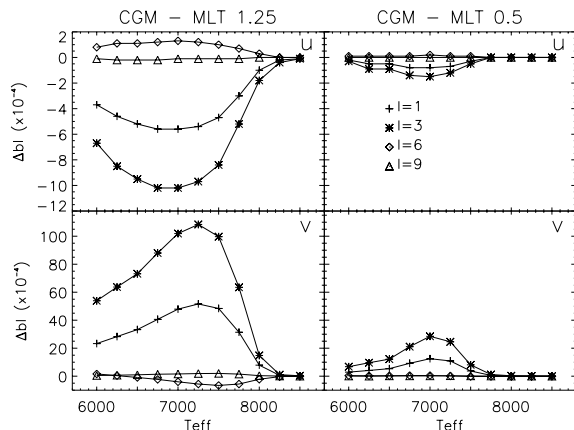


**Fig. 10.** For  $u$  (top) and  $v$  (bottom) bands and for  $\log g = 3.5$ , differences between  $b_\ell$  computed from CGM model atmospheres and  $b_\ell$  computed from MLT  $\alpha = 1.25$  model atmospheres (left) and the difference between  $b_\ell$  computed from CGM model atmospheres and  $b_\ell$  computed from MLT  $\alpha = 0.5$  model atmospheres (right), as a function of the  $T_{\text{eff}}$  for several  $\ell$  values.

As expected, larger differences are observed between CGM and MLT  $\alpha = 1.25$  than between CGM and MLT  $\alpha = 0.5$ .

A comparison with the LDC computed by Claret (2000) is made. Claret (2000) proposes a new non-linear law valid for the whole HR Diagram, however the author gives also the LDC computed from ATLAS models with the quadratic and square root laws we use in this paper. Figure 11 shows a comparison, for a given gravity, of the quadratic coefficients,  $a$  and  $b$  and square root coefficients,  $f$  and  $g$  from Claret (2000) and from this work. The general behavior of the considered LDC with effective temperature is similar for both works, i.e. a decrease of  $a$  and  $f$  and an increase of  $b$  and  $g$  with  $T_{\text{eff}}$ . This is not the case for Claret's LDC between 7500 and 8000 K where the observed discontinuity is due to the same reason mentioned in Sect. 2. The LDC values from these two works are similar at high temperatures whereas they are quite different at low temperatures. Figure 12 shows how  $I(\mu)/I(1)$  derived from the LDC from this work and from Claret (2000) matches the model atmosphere intensity. The larger differences between these two works appear at low temperature and decrease towards high temperature as also seen in LDC (Fig. 11). On the other hand, the fits are similar quality at high temperatures. We can see on these figures that the use of a higher resolution in optical depth in the model atmospheres, a different treatment of the convection and the non-use of the overshooting option in ATLAS code imply significant changes in the LDC values and then on the intensity variation with  $\mu$ .

Using model atmospheres with the CGM prescription for the convection treatment, we find that the law which gives the best results for the  $u$  band is the square root one. The cubic law gives the best fit for the  $v$  band as well as for the  $b$  band except for few models at low temperatures and high gravity. Finally, for the  $y$  band, the cubic law gives the best results for high temperatures, and the square root law for low temperatures. Similar results are generally obtained with MLT  $\alpha = 0.5$ . On the other hand, conclusions about the best law to use for a given band significantly differ when the model atmosphere

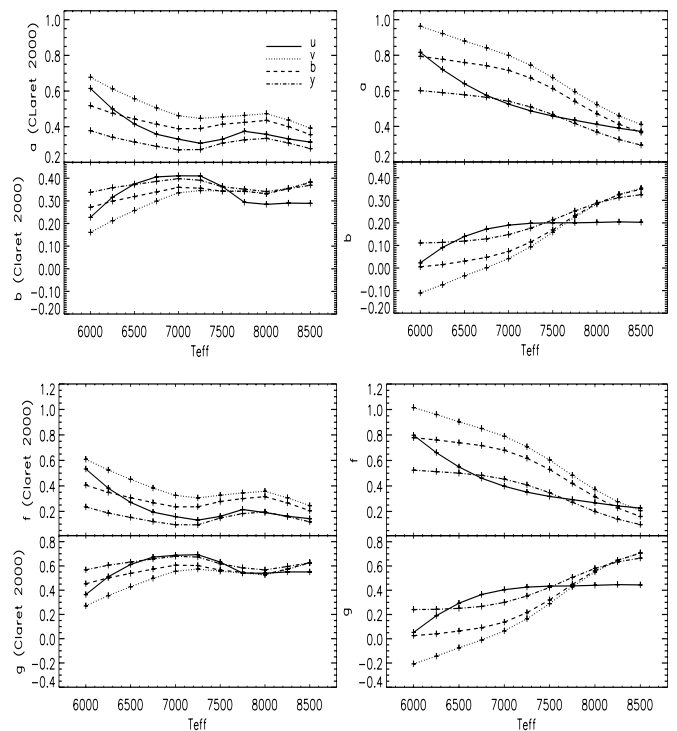


**Fig. 11.** Quadratic coefficients,  $a$  and  $b$ , and square root coefficients,  $f$  and  $g$ , from Claret (2000) (left panels) and from this work (right panels), as a function of temperature, for  $\log g = 3.5$ , for  $uby$  bands.

is computed with MLT  $\alpha = 1.25$ . For the considered temperatures and gravities and for the  $uby$  bands, similar results were obtained by Díaz-Cordovés et al. (1995) with different model atmospheres; they found by comparing a linear, a quadratic and a square root law that the latter can be a very good approximation.

The weighted limb-darkening integrals  $b_{\ell x}$  and their derivatives have then been computed from the LDC. We find, as previous authors, that the  $b_{\ell x}$  are only weakly dependent on  $T_{\text{eff}}$  and  $\log g$ . On the other hand, their derivatives significantly depend on  $\log g$  and on  $T_{\text{eff}}$ . These dependencies are  $\ell$ -dependent and differ in each  $u, v, b, y$  band. In addition, these integrals depend on the convective treatment and as expected larger differences are found between CGM and MLT  $\alpha = 1.25$  than between CGM and MLT  $\alpha = 0.5$ .

The new grid of model atmospheres which are finer spaced in temperature and gravity and have a higher resolution in the temperature distribution with depth allowed us to have smoother  $b_{\ell x}$  and their derivatives as required for the mode identification method. The improvements of these integrals and its derivatives become evident when comparing the present results with plots shown in Garrido (2000). In particular, the discontinuities in these integrals, of the order of 0.01 in absolute value translating into a few percent for the lower  $\ell$ -values but up to 30–40% for  $\ell = 4$  and even larger for higher  $\ell$ -values, have disappeared completely. Subsequently the discontinuities in the derivatives with respect to temperature, with uncertainties of several orders of magnitude, have also disappeared. We think the effect was due to the inclusion of overshooting in the

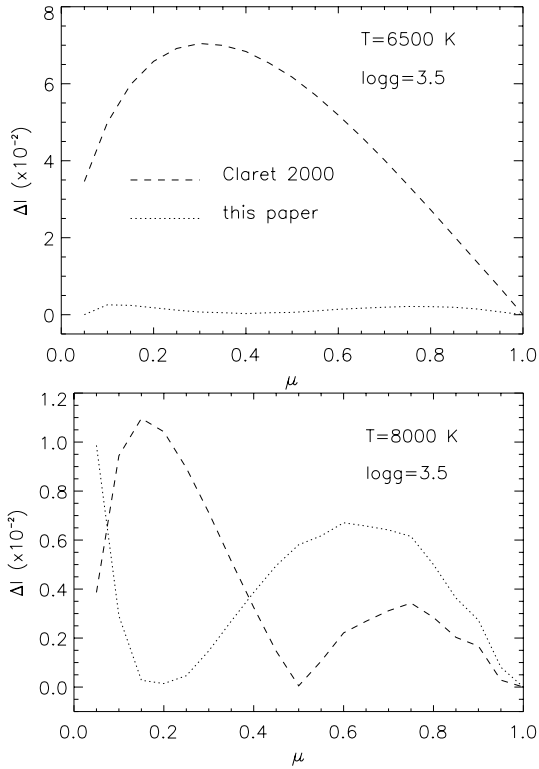


**Fig. 12.**  $\Delta I \equiv |I(\mu)/I(1) - I(\mu)/I(1)_{\text{law}}|$  for a square root law using LDC from this work (dotted line) and LDC from Claret (2000) (dashed line) for the  $u$  band,  $\log g = 3.5$ , for  $T_{\text{eff}} = 6500$  K (top) and for  $T_{\text{eff}} = 8000$  K (note the difference of vertical scale between the two, upper and lower, plots).

former calculations. The consequences on the mode identification photometric technique depends critically on the  $\ell$ -value considered and on the color index, but their contributions increase almost monotonically with  $\ell$ , as can be seen in Fig. 11 of Garrido (2000). More detailed calculations, taking into account non-adiabatic theoretical calculations to be included in the linear formula given in Watson (1988), will be given in a forthcoming paper.

Tables for all numerical coefficients are available upon request; tables for quadratic, cubic and square root LDC and the  $\sigma$  corresponding to the law for CGM models and for  $u$ ,  $v$ ,  $b$ , and  $y$  bands are available on [http://dasgal.obspm.fr/~barban/Limb\\_AF/](http://dasgal.obspm.fr/~barban/Limb_AF/)

**Acknowledgements.** The authors want to thank A. Claret for providing via CDS his LDC values and for interesting remarks and comments. CB is supported by NASA grant NAG5-11703. CB thanks B. Mosser for his financial support and T. Corbard for helpful discussions. FK acknowledges support by the Fonds zur Förderung der wissenschaftlichen Forschung (project *P13936-TEC*) and by the UK Particle Physics and Astronomy Research Council under grant PPA/G/O/1998/00576 and is grateful for the hospitality received at the Observatoire de Paris/Meudon during part of this work. UH is supported by NSF grant AST-0086249. RG acknowledges financial support from the program ESP2001-4528-PE.

## References

- Allen, C. W. 1973, *Astrophysical Quantities*, 3rd edition (London: Athlone Press)
- Balona, L. A., & Evers, E. A. 1999, *MNRAS*, 302, 349
- Balona, L. A., & Dziembowski, W. A. 1999, *MNRAS*, 309, 221
- Barban, C., Goupil, M. J., van't Veer-Menneret, C., & Garrido, R. 2001, in *Proc. of the SOHO 10/GONG 2000 Workshop: Helio- and asteroseismology at the dawn of the millennium, 2–6 October 2000*, Santa Cruz de Tenerife, Tenerife, Spain, ed. A. Wilson, Scientific coordination by P. L. Pall., ESA SP-464, 399
- Barklem, P. S., Stempels, H. C., Allende, et al. 2002, *A&A*, 385, 951
- Breger, M., Garrido, R., Handler, G., et al. 2002, *MNRAS*, 329, 531
- Canuto, V. M., Goldman, I., & Mazzitelli, I. 1996, *ApJ*, 473, 550
- Castelli, F. 1999, *A&A*, 346, 564
- Castelli, F., Gratton R. G., & Kurucz, R. L. 1997, *A&A*, 318, 841 (erratum: 1997, *A&A*, 324, 432)
- Claret, A. 2000, *A&A*, 363, 1081
- Claret, A., Díaz-Cordovés, J., & Giménez, A. 1995, *A&AS*, 114, 247
- Claret, A., & Giménez, A. 1990, *Ap&SS*, 169, 223
- Daszynska-Daszkiwicz, J., Dziembowski, W. A., Pamyatnykh, A. A., & Goupil, M. J. 2002, *A&A*, 392, 151
- Díaz-Cordovés, J., Claret, A., & Giménez, A. 1995, *A&AS*, 110, 329
- Díaz-Cordovés, J., & Giménez, A. 1992, *A&A*, 259, 227
- Dziembowski, W. A. 1977, *Acta Astron.*, 27, 203
- Dziembowski, W. A., Balona, L. A., Goupil, M. J., & Pamyatnykh, A. A. 1998, in *Proc. of the First MONS Workshop: Science with a Small Space Telescope*, ed. H. Kjeldsen, & T. R. Bedding (Aarhus Universitet), 127
- Fuhrman, K., Axer, M., & Gehren, T. 1993, *A&A*, 271, 451
- Garrido, R., Moya, A., Goupil, M. J., et al. 2002a, *Comm. in Asteroseismology*, ed. M. Breger, 141, 48
- Garrido, R., Claret, A., Moya, A., et al. 2002b, *The 1st Eddington Workshop on Stellar structure and habitable planet finding*, ed. B. Battrick, scientific ed. F. Favata, I. W. Roxburgh, & D. Galadi, ESA SP-485, 103
- Garrido, R. 2000, *Delta Scuti and Related Stars, Reference Handbook and Proc. of the 6th Vienna Workshop in Astrophysics*, held in Vienna, Austria, 4–7 August, 1999, ed. M. Breger, & M. Montgomery, ASP Conf. Ser., 210, 67
- Heiter, U., Kupka, F., van't Veer-Menneret, C., et al. 2002, *A&A*, 392, 619
- Kurucz, R. L. 1998, <http://cfaku5.cfa.harvard.edu>
- Kurucz, R. 1979, *ApJS*, Ser., 40, 1
- Kurucz, R. 1993, *ATLAS9 Stellar Atmosphere Programs and 2 km/s grid*. Kurucz CD-ROM No. 13 (Cambridge: Mass.: Smithsonian Astrophysical Observatory)
- Matsushima, S. 1969, *ApJ*, 158, 1137
- Mazeh, T., Naef, D., Torres, G., Latham, D. W., et al. 2000, *ApJ*, 532, L55
- Milne, E. A. 1921, *MNRAS*, 81, 361
- Smalley, B., Gardiner, R. B., Kupka, F., & Bessell, M. S. 2002, *A&A*, 395, 601
- Smalley, B., & Kupka, F. 1997, *A&A*, 328, 349
- Van Hamme, W. 1993, *AJ*, 106, 209
- Van't Veer-Menneret, C., & Mégessier, C. 1996, *A&A*, 309, 879
- Van't Veer, F. 1960, *L'assombrissement Centre-Bord des Étoiles*, Doctoral thesis, University of Utrecht
- Wade, R. A., & Rucinski, S. M. 1985, *A&AS*, 60, 417
- Watson, R. D. 1988, *Ap&SS*, 140, 255